Exploration of Fragmentation Mechanisms of Yellow Split Peas during Grinding Using a Multimodal Approach

Laurène Koëgel, Reine Barbar, Adrien Réau, Bernard Cuq

applied sciences

MDPI

Article

Exploration of Fragmentation Mechanisms of Yellow Split Peas during Grinding Using a Multimodal Approach

Laurène Koëgel, Reine Barbar, Adrien Réau and Bernard Cuq *

UMR IATE (INRAE, L'Institut Agro Montpellier, Université de Montpellier), 2 Place Viala, 34060 Montpellier, France; laurene.koegel@umontpellier.fr (L.K.); reine.barbar@supagro.fr (R.B.); adrien.reau@inrae.fr (A.R.)

* Correspondence: bernard.cuq@supagro.fr; Tel.: +33-(0)4-99-61-28-60

Abstract: In the context of food and agro-ecological transitions, the development of food applications based on legume flours and plant proteins requires a mastery of grain milling. While wheat grain milling has been extensively studied and is well-mastered, legume grinding and its underlying mechanisms are still poorly understood. The aim of this work is to contribute to the study of the fragmentation mechanisms of pea grains during grinding. Experiments were carried out on hulled yellow pea grains (Kameleon variety) ground under different conditions using a ball mill (MM400, Retsch®, Haan, Germany) or a micro-cylinder mill. The results showed that the grinding of pea grains, regardless of the type of mill, produced powders characterized by particle size distribution curves with a multimodal shape. The curve analysis was performed according to a simplified deconvolution approach, taking into account different particle populations without diameter overlap. Four particle populations of different sizes were identified and correlated with specific mechanisms governing the grinding of yellow split peas. The physical and biochemical properties of the resulting powders were determined. Taking into account the proportions of the four populations within the powders, the results showed a positive correlation between the volume proportions of very fine (0–10 μm) and fine (10–55 μm) particles within the powders and the starch damage rate and the specific surface area developed, irrespective of the type of mill.

Keywords: pea cotyledons; grinding process; particle populations; fragmentation mechanisms

Citation: Koëgel, L.; Barbar, R.; Réau, A.; Cuq, B. Exploration of Fragmentation Mechanisms of Yellow Split Peas during Grinding Using a Multimodal Approach. *Appl. Sci.* **2024**, *14*, 3740. https://doi.org/10.3390/app14093740

Academic Editors: Davide De Angelis and Carmine Summo

Received: 3 April 2024
Revised: 21 April 2024
Accepted: 25 April 2024
Published: 27 April 2024

1. Introduction

Pulses have been part of the human diet since the earliest domestication of agriculture and plants and are cultivated worldwide [1]. Originally consumed as cooked hulled grains, they are also ground and used as flours or fractionated and used as enriched powders (protein concentrates/isolates). The use of legume flours and powders is often associated with the total or partial replacement of wheat flour. These flours are important levers for growth in the legume crops sector, promoting consumption through their versatile functional food potential. Compared to wheat milling, the milling of legume grains and its underlying mechanisms remain poorly understood [2] There is still little information on the process parameters associated with the production of these powders and their optimization for food applications [3], although legume flours exist for several applications [4–7].

Grinding is a unit operation that fragments material under mechanical stress. Depending on the type of mill and the desired granulometry, fragmentation is achieved by applying single or repeated stresses to the grain structure that are greater than the fracture stress of the material, at the grain or at the particle scale. Depending on the type of equipment, various mechanical stresses such as compression, impact, shear, and abrasion/attrition are promoted and cause material fragmentation and the formation of small particles. Powder properties are determined by the fragmentation mechanisms depending on the grinding equipment and its operating conditions.

Some studies have investigated the influence of the milling process on the characteristics of the resulting legume powders, either by comparing the effect of different types of mills or by modulating the milling parameters using the same mill. Most of the legume powders studied were either purchased from commercial flour manufacturers [4,8] or milled on a laboratory or pilot scale using a variety of different milling equipment [9–15]. Often, a lack of information about the grinding conditions prevented the observation of relationships between process parameters and product properties. Motte et al. (2021) [16] investigated the effect of grinding conditions using a roller mill under different configurations on the powder properties of pea and lentil grains. The grinding scheme based on reduced roll spacing between passes produced more damaged starch. Bourré et al. (2019) [4] investigated the effect of parameter settings using a knife mill with different sieve sizes on the properties of legume powders. The sieve size selected had a direct influence on the granulometric characteristics of the flours. They observed differences between the powders produced in the knife mill and commercial flour. Other studies have compared the effects of different mills [9,11,15] and their setting parameters [12,17] in order to understand the mechanisms induced in the separation of constituents during the milling process. These works mainly focused on the optimal separation of cellular components (starch, proteins) to optimize the enrichment of the powder, based on the generation of fractions or streams.

There is still a lack of studies in the literature that focus on the effects of the grinding process in order to establish relationships between the parameters of the grinding process, the fragmentation mechanisms, and the properties of the powders produced. The present work aims to contribute to the study of the fragmentation mechanisms of pea grains during grinding under different conditions. Experiments were carried out with yellow split peas ground using two different mills (ball mill and cylinder mill) under different conditions. The powders obtained were characterized in terms of their particle size distribution and their microstructure. The grinding of yellow split peas, using both types of mills, results in powders with a multimodal particle size distribution. Curve decomposition, based on a simplified deconvolution approach taking into account different particle populations without diameter overlap, allowed the identification of four particle populations of different sizes. The characteristics of each population were determined in terms of size, morphology, and volume fraction within the powders. The results were discussed in relation to the involvement of different comminution mechanisms during the grinding process.

2. Materials and Methods

2.1. Raw Materials

Whole yellow pea grains harvested in France in July 2022 were supplied by Scea La Gaillière (Villiers-en-Desoeuvre, France). In order to obtain a uniformly sized pea sample, the grains were sorted and sieved using a Rotex sieve shaker (Rotex^{TM}, Cheshire, UK) with 9 and 6 mm meshes, thus representing the size of the grains collected. The sorted grains were gently dried in a pilot hot air dryer (CS40/350 climatic chamber, CTS®, Hechingen, Germany) to a target moisture content of 13.5 ± 0.1 (g water/100 g dry matter).

The dried yellow pea grains were dehulled using a dehuller (TM05, Satake, Tokyo, Japan). The grains were then packed in airtight plastic bags (1 kg of peas per bag) and stored in a cold room at 4 °C until use.

2.2. Milling Process

Yellow split pea grains were milled according to AACC 26–32.01 [18] in a cylinder mill (MLU 202, Bühler, Uzwil, Switzerland) equipped with three breaker rolls, three reduction rolls and six sieves. After milling, six different powder streams were produced separately and recombined to obtain the whole powder. An air classifier (ATP50, Hosokawa-Alpine, Augsburg, Germany) was used to classify the powder fractions. The system was fed with 2 kg of sample at a flow rate of 0.7 kg.h^{-1}, an air flow of 99.9 m^3.h^{-1}, and a selector speed of 8000 rpm. The very fine particles (diameter < 10 µm) were separated in this first step. The remaining powder was then separated by dry sieving using a mechanical granulometer

(Rotex™, Cheshire, UK) with a column of sieves with decreasing mesh sizes (315, 280, 160, and 100 µm). To obtain the fine fraction of pea powder (10 < diameter < 75 µm), the fraction passing through the 100 µm sieve was recovered and sieved using a Hosokawa 200LS-N (Augsburg, Germany) suction sieve shaker with a 75 µm sieve. The medium fraction (75 µm < diameter < 500 µm) was obtained by remixing the fractions retained (>100 µm) by mechanical sieving and the suction sieve shaker.

2.3. Impact of Grinding Conditions

The influence of the grinding conditions was studied using two different laboratory mills. A laboratory roller mill (Micromill, UMR IATE prototype; Montpellier, France [19]) is used to generate compressive/shear stresses during the grinding process. A laboratory vibratory impact ball mill (MM400, Retsch®, Haan, Germany) in single ball configuration is used to generate mainly impact stresses during grinding.

To investigate different grinding conditions, yellow split peas were ground by modulating the setting parameters on both mills (Table 1), using a fractional factorial experimental design with 4 factors and 2 levels per factor (2^{4-1}). For each mill, a total of 8 different experimental grinding conditions were investigated (Tables 2 and 3). The ball mill was also used with a load of 10 g of yellow split peas per grinding jar, a single steel ball (diameter = 25 mm), and a grinding frequency of 20 Hz, for different grinding times (between 30 and 300 sec). It should be noted that in all trials, the grinding conditions were deliberately set after preliminary tests to minimize heating constraints. Only run 7 of the ball mill experimental design and kinetic runs longer than 4 min generated uncontrolled heating within the grinding jars, which could have affected the state of the constituents of the pea powders produced. Such effects were not evaluated in this study.

Table 1. Experimental domain explored to study the influence of the roller mill and of the ball mill setting parameters on the characteristics of the yellow pea powders produced.

Mill Setting Parameters	Natural Lower Values (coded = −1)	Natural Higher Values (coded = +1)
Roller mill		
Cylinder type: plain (P) or splined (S)	S-S-S-S	S-P-P-P
Cylinder gap reduction rate (mm)	0.9–0.6–0.4–0.05	0.9–0.2–0.05–0.05
Rapid cylinder rotation speed (rpm)	400	800
Speed differential	1.33	2.5
Ball Mill		
Grinding time (min)	1	4
Ball diameter (mm)	20	25
Grinding frequency (Hz)	20	30
Product mass per jar (g)	5	10

Table 2. Roller mill experimental design.

Essays	Factor 1 (F_1)	Factor 2 (F_2)	Factor 3 (F_3)	Factor 4 (F_4)
e1	S-P-P-P	0.9–0.6–0.4–0.05	400	1.33
e2	S-S-S-S	0.9–0.2–0.05–0.05	400	1.33
e3	S-S-S-S	0.9–0.6–0.4–0.05	800	1.33
e4	S-P-P-P	0.9–0.2–0.05–0.05	800	1.33
e5	S-S-S-S	0.9–0.6–0.4–0.05	400	2.5
e6	S-P-P-P	0.9–0.2–0.05–0.05	400	2.5
e7	S-P-P-P	0.9–0.6–0.4–0.05	800	2.5
e8	S-S-S-S	0.9–0.2–0.05–0.05	800	2.5

F_1 = cylinder type; F_2 = cylinder gap reduction rate (mm); F_3 = rapid cylinder rotation speed (rpm); F_4 = speed differential.

Table 3. Ball mill experimental design.

Essays	Factor 1 (F_1)	Factor 2 (F_2)	Factor 3 (F_3)	Factor 4 (F_4)
e1	4	20	20	5
e2	1	25	20	5
e3	1	20	30	5
e4	4	25	30	5
e5	1	20	20	10
e6	4	25	20	10
e7	4	20	30	10
e8	1	25	30	10

F_1 = grinding time (min); F_2 = ball diameter (mm); F_3 = grinding frequency (Hz); F_4 = product mass per jar (g).

All grinding conditions were performed at least in triplicate.

2.4. Particle Size Characterization of the Powders

Particle size analysis of the powders was performed at room temperature using a dry laser diffraction particle size analyzer (LS 13 320 XR, Beckman & Coulter®, Brea, CA, USA). A sample of approximately 2 g was characterized for each powder. The cell rotation speed was set at 70% to allow product suspension and circulation through the cell. The refractive index was set at 1.49. The particle size distribution of the powders was described by plotting the volume fraction (%) of the particles as a function of particle size (μm) and by calculating the median diameter (d_{50}; μm). The particle size distribution curves of the powders were analyzed by deconvolution using four log-beta laws to describe the 4 populations of particles of different sizes. Each population of particles is delimited by a minimum and a maximum diameter value. The volume fraction (%) and the median particle diameter (d_{50}; μm) of each of the 4 particle populations were calculated. Measurements were performed in triplicate.

2.5. Scanning Electron Microscopy (SEM)

SEM was used to describe the cellular structure of the pea cotyledon and the morphology of the 4 different particle populations. Observations were made using a bench-top scanning electron microscope (SEM) (Phenom ProX, Phenom-World BV®, Eindhoven, The Netherlands). Cotyledon sections and powders were mounted on a support and held in place with double-sided carbon tape. For each sample, the support was mounted on a rack for insertion into the machine. The samples were observed directly, without metallization. The following observation parameters were set: 10 kV acceleration voltage, image mode. The 1024 × 1024-pixel images are of high quality, resulting in fast acquisition times. Magnifications ranging from 50 to 300 μm were used. To observe the cell structure, five pea cotyledons were sectioned perpendicular and parallel to the embryo axis. The average cell size was estimated from cotyledon sections with intact cells. Since the sectioning protocol was simplified (no cryopreservation), cell damage (open cells) can be expected. Mean values were estimated from 20 different measurements. For starch granule observation, images were selected based on a qualitative observation of samples taken from whole grain sections and powders containing free, intact starch granules. The average starch granule size was determined from 70 random measurements of granule length (oval shape) observed on different images.

2.6. Evaluation of Flowability of Pea Powders Using the Hausner Ratio

The aerated densities of the powders were determined in triplicate by pouring a known mass of approximately 100 g of sample into a 250 mL graduated glass tube, inclined at 45° to allow free flow of the powder. From the measurement of the volume occupied by the powder (V_0) and knowing of the initial mass (m), the aerated density (ρ_a) can be determined (Equation (1)).

$$\rho_{a=\frac{m}{V_0}}, \quad (1)$$

Tapped densities were measured in triplicate using an automated tapped density analyzer (Autotap AT-6-220-50, Quantachrome Instrument®, Boynton Beach, FL, USA) capable of approximately 250 falls.min^{-1} from 3 mm. The same samples were tested as for the aerated density measurements. As there are no standards for measuring the bulk density of legume flours, the packing kinetics up to 3 constant volume measurements was chosen. The tapped density is calculated using Equation (2), where m is the mass of the beaker and V_f is the final volume occupied by the powder after compaction.

$$\rho_{t=\frac{m}{V_t}}, \quad (2)$$

From measurements of the apparent uncompacted volume (V_0, cm^3) and the final compacted volume (V_T, cm^3) of the powders, the Hausner index, which is representative of the interparticle friction limiting the flow, was calculated using Expression 3 [20], where ρ_t = tapped density and ρ_a = aerated density. A Hausner index below 1.2 was considered to indicate high flowability.

$$\text{Hausner ratio}_{=\frac{\rho_t}{\rho_a}}, \quad (3)$$

2.7. Measurement of the BET Surface Area

The specific surface area was measured by the Brunauer–Emmett–Teller (BET) method based on nitrogen absorption using the Porosity and Surface Analyzer (ASAP 2460, Micromeritics®, Norcross, GA, USA). The principle of the method is based on the measurement of the solid–gas interface surface area per unit sample mass. The samples were first degassed at 50 °C for 48 h (VacPrep061, Micromeritics®, USA). The samples were cooled with liquid nitrogen during the measurement.

2.8. Color Analyses

The color values of yellow split pea powders were measured using a chromameter, CR-410 (Konica Minolta, Tokyo, Japan), and reported in the CIE color space (L*, a*, and b*). Measurements were made in triplicate.

2.9. Starch Damage Content in Powders

Starch damage was determined according to AACC method 76–31.01, with the Megazyme K-SDAM kit (Megazyme; Wicklow, Ireland). Measurements were performed in triplicate.

2.10. Statistical Analysis

Means and standard deviations were calculated from triplicates for all measurements except for BET, which was performed in duplicate. Only mean values are shown on charts for clarity purposes while ensuring that all data respect a coefficient of variation of less than 5%. Full information is available upon request. Analysis of variance by Tukey's multiple comparison range test was performed at the 5% significance level.

3. Results

3.1. Cotyledon Matrix Microstructure

The microstructure of the pea cotyledon has been described by SEM. At the tissue scale (Figure 1a), the cotyledon structure is formed by the assembly of cells of apparent polyhedral shape, bounded by sheet-like cell walls. The apparent diameter of the cells was estimated from multiple size measurements on different images (84 ± 13 µm). The highly ordered cells could be associated with a "honeycomb-like model material" based on the tissue structure of wheat [21]. The fiber-rich cell walls are clearly visible. Similar microstructural descriptions of pea cotyledons have been reported [22–24].

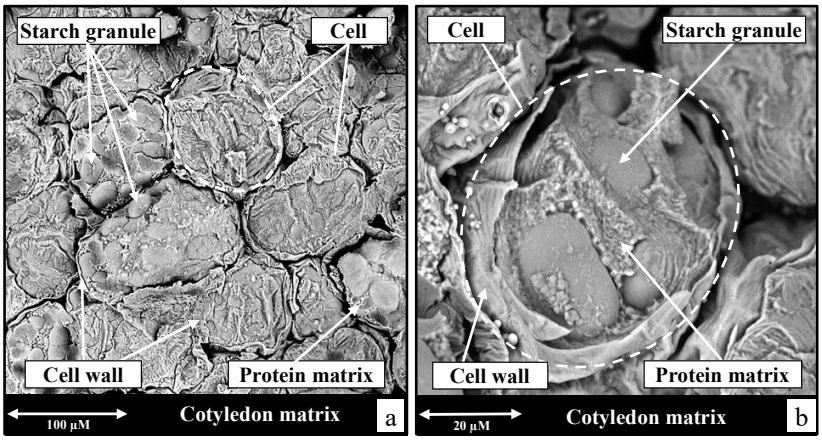

Figure 1. Scanning electron micrographs of pea cotyledon structure. (**a**) Cotyledon matrix structure; (**b**) cotyledon cell structure.

At the intracellular scale (Figure 1b), the cell structure could be described as a dense collection of different cohesive granular structures. This confirms observations already made in the literature [14,25]. The cell interior consists of elongated starch granules embedded in a matrix rich in small protein bodies, recognizable by their round shape and small size (1–4 µm). The apparent length of the starch granules was estimated from several images (24 ± 7 µm). A similar description of the structure of pea cells has been reported [22,26]. The heterogeneous nature of intracellular contents (i.e., polydisperse starch granules entangled in a protein matrix) may imply different stress resistance (i.e., failure threshold) during milling. The cell wall thickness of the legume cotyledon influences the grinding behavior [2,27]. Legumes with thicker cell walls are more friable during milling. The mechanisms involved in cotyledon grinding behavior may be influenced by the properties of the cell contents and cell walls, as well as the cohesion between the cell walls and their components (starch granules and proteins).

3.2. Particle Populations in Pea Powders

Regardless of the type of mill and the grinding conditions, the grinding of pea cotyledons produces powders with a wide range of particle diameters between 1 and 2000 µm. The particle size distribution curve for the pea powders shows a multimodal shape, characterized by several peaks of different intensity depending on the grinding conditions. This trend was observed for the powders generated by the two experimental designs with ball and roller mills, as well as for the grinding kinetic with the ball mill (Figure 2). Multimodal particle size distributions of legume powders, especially pea powders, have already been reported in the literature [8,28,29].

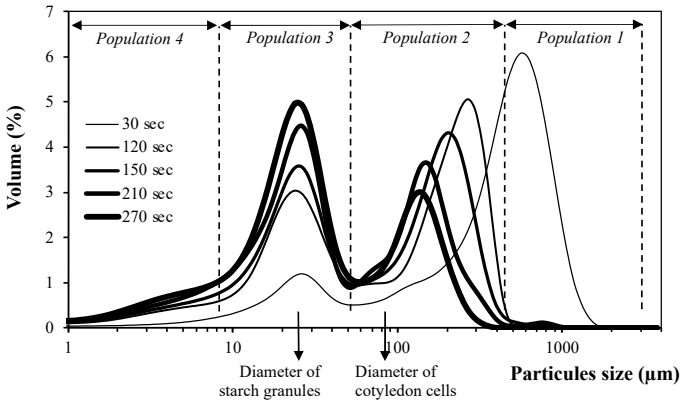

Figure 2. Particle size distributions of pea powders at different grinding times in the ball mill.

The particle size distribution of the powders (Figure 2) was studied as a function of the grinding time using the ball mill. The effect of grinding time can be seen in the evolution of peak intensities. The intensity of peaks associated with coarser particle size ranges decreases with increasing grinding time, while the intensity of peaks associated with finer particle size ranges increases (Figure 2).

We propose an original approach to the analysis of multimodal distribution curves, considering that pea powders are formed by the coexistence of several particle populations, differentiated by their diameters and their characteristics. Bordeaux et al. (2006) [30] proposed a probabilistic deconvolution method for the analysis of multimodal particle size distribution curves of powders obtained after the milling of durum wheat grains. Their probabilistic solutions considered 4–5 particle populations to deconvolute the particle size curves, with overlapping diameters between the populations. However, they did not identify relationships between the different populations and the comminution mechanisms. In the present study, the multimodal analysis is based on a simplified approach by considering the assembly of particle populations without diameter overlap. We assume that each of the log-beta laws identifiable on the particle size distribution curve can be associated with a specific population of particles within the powder. The decomposition of the particle size distribution curves by deconvolution of several log-beta laws allows us to identify four different populations whose presence is either systematic (i.e., in all powders) or dependent on the grinding conditions. This method made it possible to identify the limits for each population (as described in the next section). However, in the case of population 2, we chose to define the upper limit as a technological value with the maximum particle size of standard quality wheat semolina (~470 µm). This criterion was chosen as the boundary between populations 1 and 2.

The multimodal analysis makes it possible to identify the different populations of particles in the pea powders in order to describe the specificities of their microstructure (Figure 2).

(i) Population 1 is associated with very large particles with a diameter greater than 470 µm (Figure 2). This population is made up of preground particles that are usually considered too large for classical technological applications. Particles of population 1 consist of large tissue fragments of the cotyledon matrix with a high proportion of intact cells and only a few open cells in the periphery (Figure 3a). The diameter range of the very large particles (>470 µm) is largely higher than the diameter of the cotyledon cells (84 µm).

(ii) Population 2 is associated with coarse particles with diameters ranging between 55 and 470 µm (Figure 2). This particle diameter range is classically suitable for technological food applications of pea powders as flour and/or semolina. These particles are mostly composed of small fragments of cotyledon matrix with a high proportion of open cells exposing the cell contents and intact cells exposing the cell walls (Figure 3b). The diameter of the cotyledon cells (84 µm) is within the diameter range of coarse particles (55 and 470 µm). This population has not been specifically identified in the literature for powders derived from legume grinding. This population is characterized by a wide range of diameters, since the multimodal curve analysis did not isolate different populations between 55 and 470 µm. However, population 2 could contain several subpopulations whose presence is not systematic in the powders under the grinding conditions studied. Some of the powders produced are represented by population 2 with a more limited range of particle sizes (which does not go as far as 470 µm).

(iii) Population 3 is associated with fine particles between 10 and 55 µm in diameter (Figure 3). The fine particles are mainly composed of whole or damaged free starch granules (Figure 3c), cell fragments, clumps of cell material, and/or reduced fragments of cell walls. The apparent diameter of starch granules (24 µm) is in the range of fine particle diameters (10–55 µm) and is smaller than the diameter of cotyledon cells (84 µm). Similar fine particles have been observed after pea milling [23,27,31].

(iv) Population 4 is associated with very fine particles with diameters between 1 and 10 µm (Figure 2). This population is heterogeneous and includes small protein bodies, cell debris, clumps of cell material or fragments of cell walls (Figure 3d). This population has previously been identified in powders derived from pea milling [9,23]. It may also contain small starch granules [22,31] or fragments of damaged starch. The apparent diameter of starch granules (24 µm) is higher than the diameter range of very fine particles (1–10 µm).

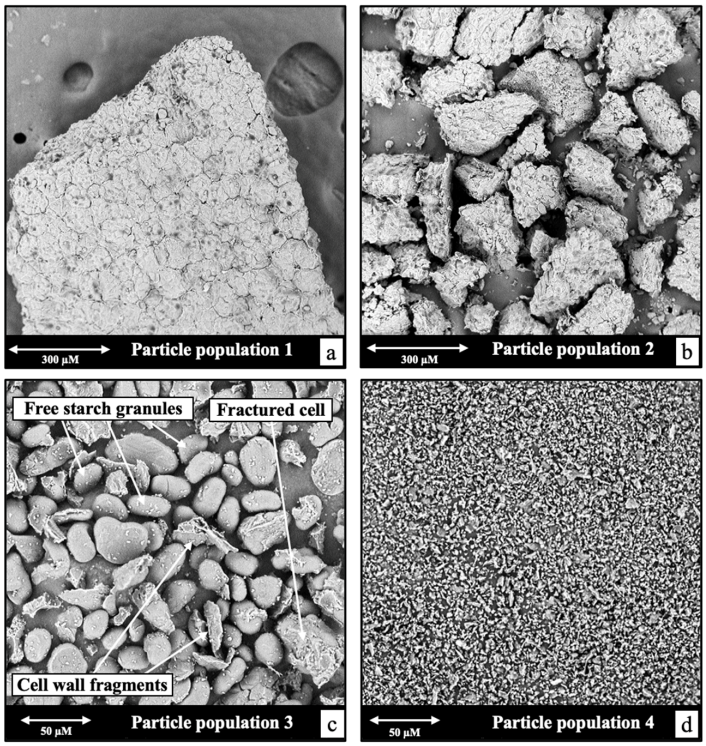

Figure 3. Scanning electron micrographs of particle populations of pea powder cotyledon structure; (**a**) particle population 1; (**b**) particle population 2; (**c**) particle population 3; and (**d**) particle population 4.

Regardless of the grinding conditions, populations 2, 3, and 4 are systematically present (Figure 4) in the pea powders produced.

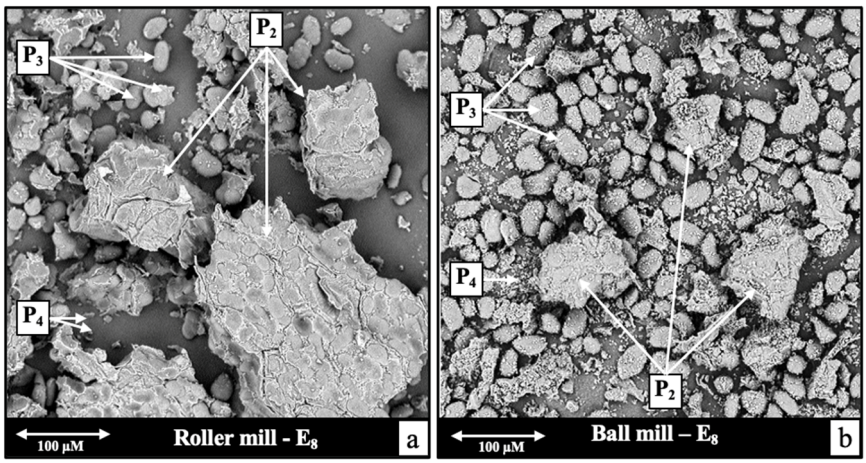

Figure 4. Scanning electron micrographs of particle populations of two pea powders produced by a roller mill (**a**) and a ball mill (**b**), where population 2 = P_2; population 3 = P_3; and population 4 = P_4.

3.3. Effect of Grinding Time on the Particle Size Distribution Curves

The particle size distribution of the powders (Figures 2 and 5) was studied as a function of the grinding time using a ball mill. The very large particles (population 1) are present in the powders only under moderate grinding conditions (i.e., short duration). This corresponds to pregrinding conditions.

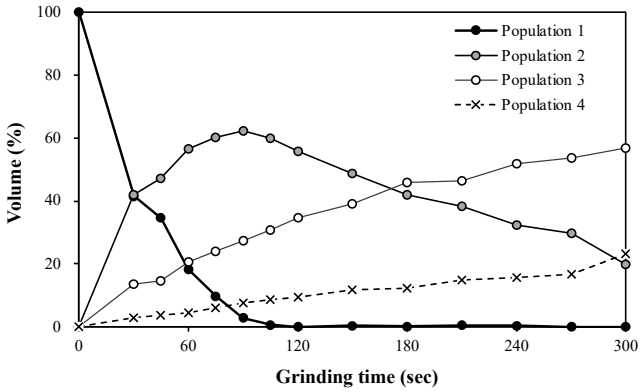

Figure 5. Population volume proportions of pea powders at different grinding times in the ball mill.

The results show that increasing the grinding time in the ball mill induces significant changes in the granulometric distribution curve (Figure 2), and in the volume fractions of the four populations (Figure 5), with a decrease in the coarsest population (population 1), an increase, stagnation, and then decrease in population 2, and a continuous, monotonic increase in populations 3 and 4.

Under these grinding conditions, after 30 s of treatment, the very large particles (population 1) are still very present, representing about 40% by volume of the powder. As the grinding time is increased, their frequency decreased exponentially. After 120 s, the presence of very large particles (population 1) is "residual".

The frequency of coarse particles associated with population 2 (<55–470 µm) shows a particular curve pattern that can be divided into two phases:

Phase 1: A first phase up to 90 s, in which the increase in grinding time leads to an increase in their frequency in the powder. This phase, which could be described as a growth phase, could be explained by the presence of a large proportion of the coarse population (population 1) at the start of the grinding, which feeds the production of the coarse particles. At the same time, two other phenomena occur:

(i) The fragmentation of the population 1 particles generates the release of smaller fragments (or cellular components).
(ii) The particles of the population already generated within population 2 are also reduced in some cases.

Both mechanisms increase the frequency of populations 3 and 4.

Phase 2: From 90 s, the increase in grinding time leads to a decrease in its frequency in the powder. This phase, associated with its decay, highlights the fragmentation of population 2 as the dominant mechanism feeding the frequency of populations 3 and 4. These populations, as defined in our study, could therefore be described as a "transfer" populations. However, the release of components or the parallel fragmentation of the already generated population 2 remains a minor phenomenon from the point of view of volume yield, hence this growth phase. At the end of the grinding process, this population remains at around 20% in relative terms.

From the early stages of grinding and throughout the process, the volume proportions of fine particles (populations 3 and 4) follow an increasing trend (i.e., power law). The rapid and simultaneous formation of these fine particles, especially population 3 associated with free starch granules, suggests that the starch granules adhere poorly to the intracellular matrix.

In contrast to the coarsest particle populations (populations 1 and 2), whose median size varies with grinding time or conditions, populations 3 and 4 have a relatively stable median size regardless of grinding conditions or duration (indicated in Figure 2 by the granulometric stability of the peaks in the corresponding particle size range).

This difference suggests that subcellular components are not subject to classical fragmentation mechanisms when released within powders, as indicated by the relative stability of the median diameter of populations 3 and 4 across all tests.

With regard to populations 3 and 4, it should be noted that the frequency expression is described in terms of volume, which reduces the effect for populations with fine granulometry compared to their expression in numbers. In addition, these populations (possibly including population 4 to a greater extent) could adopt association mechanisms (agglomeration and/or surface adhesion to other particles), which could lead to a bias in their expression. The observed slopes certainly underestimate the physical reality of the phenomena.

3.4. Effect of Grinding Conditions on the Particle Size Distribution Curves of the Mill

The volume proportion of the four populations in the powders varies according to the type of mechanical stress during grinding (roller mill and ball mill) and to the setting parameters (Figure 6). The results show significant differences between the two mills used. The very large particles (population 1) are only present only under certain grinding conditions associated with moderate pregrinding intensities. In all tests with the roller mill (Figure 6a), the coarse particles (population 2) are the major fraction (volume fraction > 50%). This is at the expense of the fine (population 3) and very fine (population 4) particles. In all of the ball mill tests (Figure 6b), the proportions of population 3 particles are more balanced, with significant diversity depending on the mill settings. Populations 2 and 3 are the most common, with a lower proportion of population 4 particles. The proposed experimental design, using two different types of mills, has produced powders with significant differences between the volume proportions of the four populations.

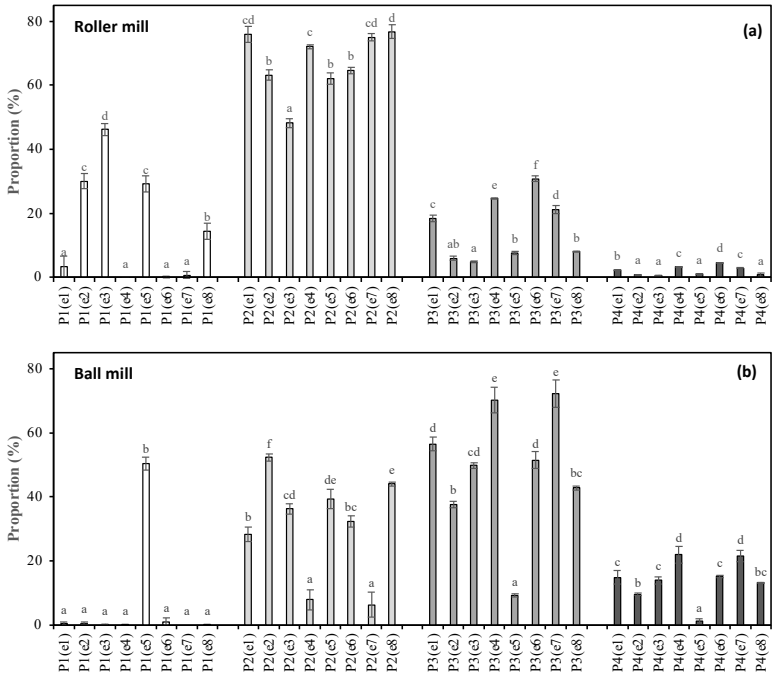

Figure 6. Proportion (%) of the four different particle populations of different pea powders ground (**a**) with a roller mill and (**b**) a ball mill (P1 = population 1; P2 = population 2; P3 = population 3; P4 = population 4) under different grinding conditions. Values with different letters in the same particle population fraction are significantly different ($p < 0.05$). Please refer to Tables 2 and 3 for details of grinding conditions e1 to e8 for roller mill and ball mill essays, respectively.

Ball milling also appears to produce a higher proportion of fine particles (populations 3 and 4) than roller milling (Figure 6).

With regard to the characterization results obtained in terms of cell structure dimensions of pea cotyledons, it can be assumed that under our grinding conditions, the following are true:

- Compression/shear grinding (combined with roller milling) is more likely to have preserved the cellular integrity of the cotyledons due to its coarser particle size (i.e., producing powders with particles predominantly associated with population 2 (Figure 6), grouping together particles of sizes larger than the cell size).
- Impact grinding (combined with ball milling) produced a higher proportion of cell fragments (Figure 6) associated with open cells and the release of subcellular components (i.e., a high proportion of particles < 55 µm (population 3) within the powders produced).

3.5. Mechanisms Involved in the Grinding of Pea Cotyledons

Analysis of the effect of grinding conditions on the particle size distribution of the powders allowed a phenomenological model to be proposed that combines several mechanisms that can occur simultaneously and/or sequentially.

(1) Cotyledon fracture (crack initiation and propagation): Cotyledon fracture is the first step in the comminution of the cotyledon matrix. Pea cotyledon fracture results in the simultaneous formation of several particle populations, with a very high proportion of very large particles (population 1) and a lower proportion of coarse (population 2), fine (population 3), and very fine (population 4) particles (Figure 5). Under the mechanical stresses induced by the mill, cracks form and propagate in the cotyledon, initiating fragmentation. The fracture planes generated in the cotyledon depend on the intrinsic mechanical properties of the structure and the presence of structural discontinuities. Under intense grinding conditions (or long grinding times), the very large particles (population 1) are not present in the powders produced as they are converted to coarse particles (population 2) by fragmentation mechanisms. The formation of population 1 and 2 particles creates surfaces that expose cellular structures and their contents [32].

(2) Particle fragmentation (size reduction and surface generation): Fragmentation mechanisms are associated with the formation of a fracture plane within the core of the very large particles, resulting in the formation of coarse particles (population 2). The median diameter of the coarse particles (100–300 µm) is larger than the mean cell size (84 µm) in the pea cotyledon. Two different fracture behaviors can be distinguished. (i) Fracture propagation along weak lines of the matrix tissue, following the organization of the cell walls, produces particles with intact cells. (ii) Fracture propagation through the cell matrix without following the organization of the cell walls produces particles with open cells at the surface exposing their contents. The grinding process combines these two fragmentation mechanisms [21]. The fragmentation mechanisms induce a significant decrease in the particle diameter of the coarse particles (population 2), as described by the shift in the peak of the volume proportion (Figure 2). The position of the fracture planes in the cotyledon structure determines the elements that can be exposed (or not) on the surface of the generated particles, which can be either cell walls (closed cells) or cell contents (open cells).

The size reduction mechanism can be monitored by examining the median diameter (d_{50}) of population 2 across all grinding trials. The peak shifts observed in Figure 2 reflect a decreasing trend in the median diameter of the particles in population 2, suggesting that the grinding time has an effect on the median particle diameter of population 2. The median diameter results for this population across all trials highlight the classic fragmentation mechanism associated with a progressive reduction in median particle size. Each grinding trial is associated with a "state" of fragmentation mechanism progression that results in a median particle size specific to the grinding time of that population. Monitoring

the median size of coarse populations could be an indicator of the progression of the fragmentation mechanism.

The relationship between the volume proportion and mean diameter of population 2 particles depends on the type of mill and grinding conditions (Figure 7).

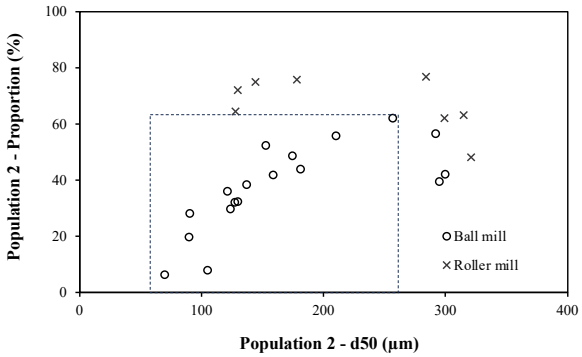

Figure 7. Fragmentation mechanism represented by the change in volume proportion change of population 2 as a function of its d_{50} change under different grinding conditions.

The fragmentation of population 1 feeds the presence of population 2 and monitors the behaviors of the two populations.

On the one hand, for impact grinding (highlighted zone in Figure 7), we can observe that the decrease in the diameter of population 2 particles correlates with the decrease in their proportion. The increase in grinding intensity favors the degradation of population 1 particles, resulting in a rapid reduction in their proportion in the powder. In this case a major fragmentation process occurs for population 2, in the absence of population 1, which contributes to this phenomenon.

On the other hand, outside of this zone, and for certain ball and roller milling, the reduction in the diameter of population 2 particles does not correlate with their proportion. This lack of correlation highlights the existence of a concomitant mechanism whereby both population 1 and population 2 are fragmented.

(3) Cell wall delamination: Analysis of the microscopic images of the powders allows the identification of isolated large cell wall fragments (Figures 3c and 8a,b) which could be associated with a possible cell wall delamination mechanism. The cotyledon cells located on the surface of the generated particles exposed their cell wall, which could be separated when subjected to mechanical stress. This possible delamination mechanism suggests weak cohesion between cell walls and cell contents. Isolated large fragments of cell walls were observed in all powders, irrespective of the type of mechanical stress.

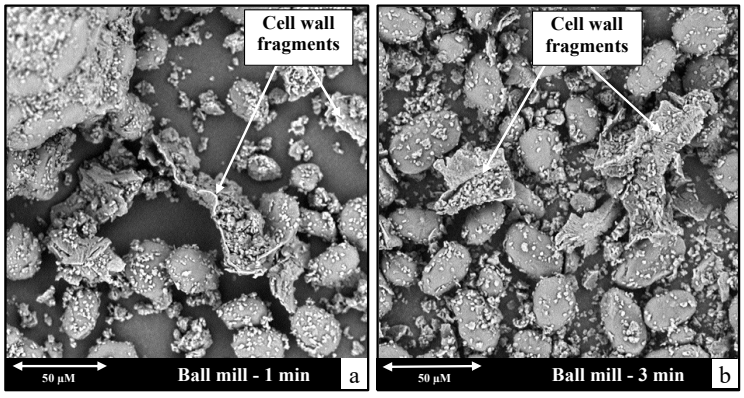

Figure 8. Scanning electron micrographs of two pea powders from ball milling kinetics; (**a**) pea powder ground with the ball mill during 1 min; (**b**) pea powder ground with the ball mill during 3 min.

(4) Release of subcellular components: The increase in exposed specific surface area of coarse particles of population 2 results in the greater exposure of cellular structures on the particle surface. The presence of open cells on the particle surface exposes the cell contents, particularly the starch granules. The decrease in the median diameter of population 2 particles correlates with the increase in the proportion of the fine particles (population 3) (Figure 9). The exposure of starch granules on the generated surface allows the expression of a release mechanism for loosely attached starch granules. In the pea cotyledon, starch granules are weakly attached to the protein matrix [29,32] and can be easily released under the mechanical stress of the grinder. For an equivalent value of the median diameter (d_{50}) of population 2, the release of starch granules depends on the type of mill (Figure 9). The ball mill, which is mainly based on impact stresses, is more effective at releasing starch granules than the roller mill, which is based on compression and shear stresses. This difference may be explained by greater intercellular fragmentation during impact grinding, which facilitates the release of subcellular components. It can be assumed that roller milling favors fragmentation of the cell surface, thus limiting the exposure of intracellular contents and the release mechanism of subcellular components. SEM observations of the fine particle powder showed free starch granules whose elongated shape was preserved, suggesting that the granules were not fragmented during grinding (Figure 3c). It is also possible that a small proportion of population 3 consists of "small" fragments of cell structures resulting from the fragmentation mechanism (i.e., small particles from population 2).

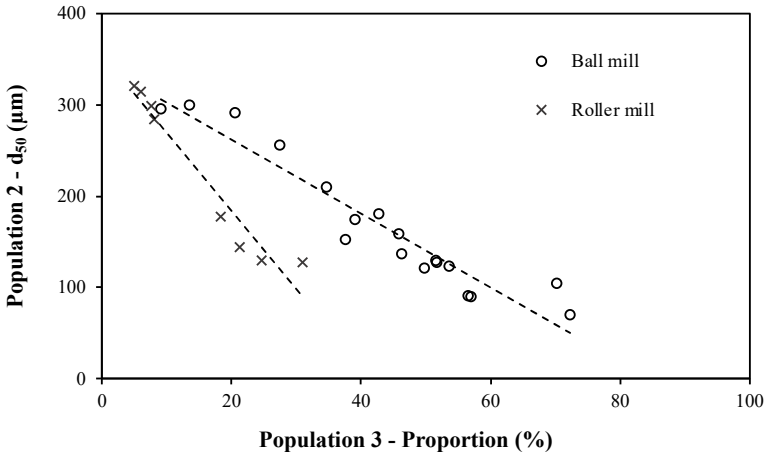

Figure 9. Subcellular component release mechanism represented by the d_{50} change of population 2 as a function of the volume proportion change of population 3 under different grinding conditions.

(5) Particle erosion: During the grinding process, regardless of the type of mill, there is a great deal of friction, resulting in abrasive stresses and erosion mechanisms. These mechanisms cause the formation of a fracture plane at the periphery of all the particles. These mechanisms do not significantly change the particle diameter but produce a large number of very fine particles (population 4). The very fine particles are composed of small fragments of the structured cell parts (walls, protein matrix, etc.) of the cotyledon. Depending on its proportion in the native pea cotyledon and its ability to resist abrasion, each component of the cotyledon cell represents a greater or lesser proportion of the debris within the population 4 [21]. Under our grinding conditions, the abrasion mechanism of the surface of the fine particles (population 3) is described by the correlation between the slight reduction in the median diameter of population 3 and the increase in the starch damage rate (Figure 10) or the increase in the proportion of very fine particles (Figure 11). These mechanisms occur quasi-simultaneously with the fragmentation mechanism of population 2, as a result of the release mechanism by disentangling matrix protein bodies upon exposure [9,23].

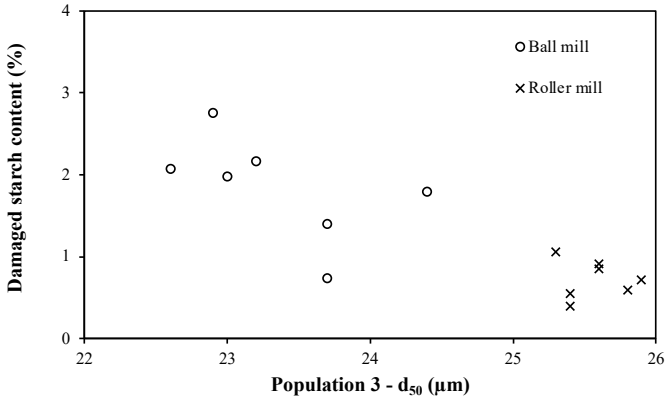

Figure 10. Effect of the median diameter (d_{50}) of population 3 particles on the damaged starch content of the powders.

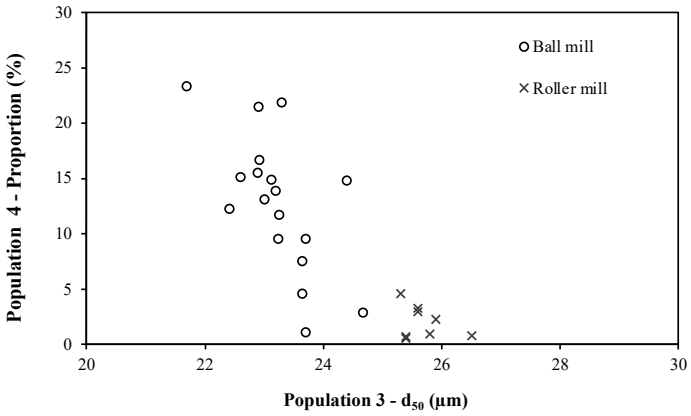

Figure 11. Effect of the median diameter (d_{50}) of population 3 particles on the proportion of population 4 particles.

3.6. Effect of Grinding on Powder Characteristics

3.6.1. Effect on Exposed Surface Area and Flowability

As expected, a power law describes the relationship between the median particle diameter and particle surface area. The changes in the specific area of coarse particles (population 2) as a function of the proportion of populations 3 and 4 (Figure 12) show that the surface area of the coarse particles produced is related to the exposure of constituents involved in both starch granule release and cellular constituent erosion.

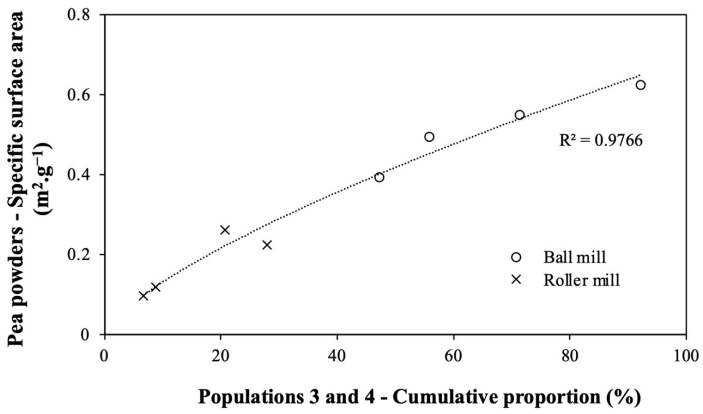

Figure 12. Effect of the cumulative proportion (%) of population 3 and 4 particles on the specific surface area ($m^2.g^{-1}$) of pea powders.

The increase in specific surface area within powders can have an impact on their functionality, particularly in terms of flowability as assessed by the Hausner ratio. The proportion of fine (population 3) and very fine particles (population 4) is positively correlated with the Hausner ratio (Figure 13). As the number of fine and very fine particles increases, the contact area between the particles increases, resulting in greater cohesion forces between the particles and lower flowability. The powders produced by the experimental design roller mill produced a lower proportion of fine particles (populations 3 and 4) compared to the powders produced by the ball mill, which are composed of a high proportion of fine particles (Figure 6). The presence of populations 3 and 4 in the powders is mainly related to the release mechanism of subcellular components. The results suggest that this mechanism is a limiting factor in the fluidity of pea powders.

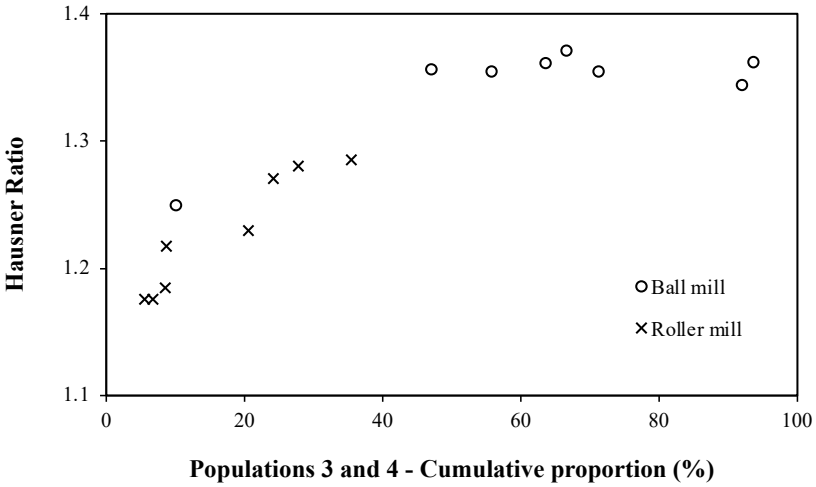

Figure 13. Effect of the cumulative proportion of population 3 and 4 particles on the flowability of powders.

Some of the very fine particles can also adhere to the surface of the larger particles (Figure 14), leading to a higher surface roughness, which causes higher friction and limits the flow behavior. Frictional forces depend on both the chemical nature of the particles and their surface properties. When comparing flow index values, ball-milled powders have a poor flow index due to a higher proportion of population 3 and 4 particles.

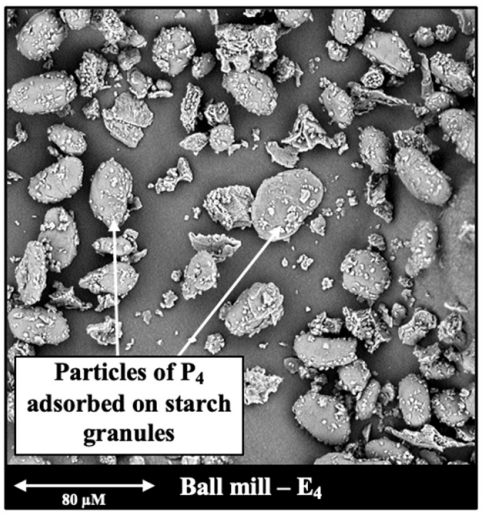

Figure 14. Scanning electron micrographs of a pea powder from ball milling tests.

3.6.2. Effect on Powder Colors

As expected and already reported in the literature, the increase in lightness (L*) and the decrease in the red (a*) and yellow (b*) indices of powders correlate with the decrease in particle size [14,33–35]. The evolution of lightness as a function of the median diameter of pea powders is specific to the type of mill (Figure 15). The finer the particles, the greater the surface area developed, resulting in more light being reflected and thus an increase in lightness L*. This difference is more pronounced for larger particle sizes than for smaller ones.

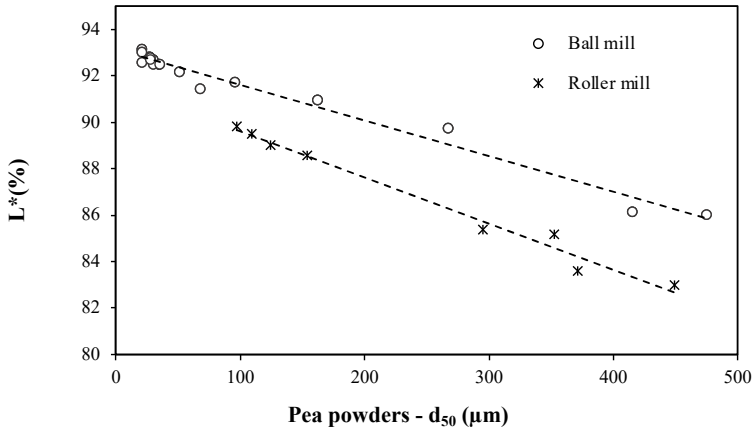

Figure 15. Influence of the mean diameter (d_{50}) of pea powders on their lightness.

However, in order to study the additional effect of the fine particle populations (P_3 and P_4) generated by the grinding configurations, we propose to plot the proportion of population 3 and 4 particles as a function of lightness, which is superimposed irrespective of the type of mill (Figure 16). The curves are exponential and converge to a finite value above 60% of particles with a diameter below 55 µm. Powder lightness is influenced by the cumulative proportion of population 3 and 4 particles within the powders, which is dependent on the type of stress. Further investigation is needed in order to link the physical characteristics of powders like colors to the physicochemical and biochemical properties of each population.

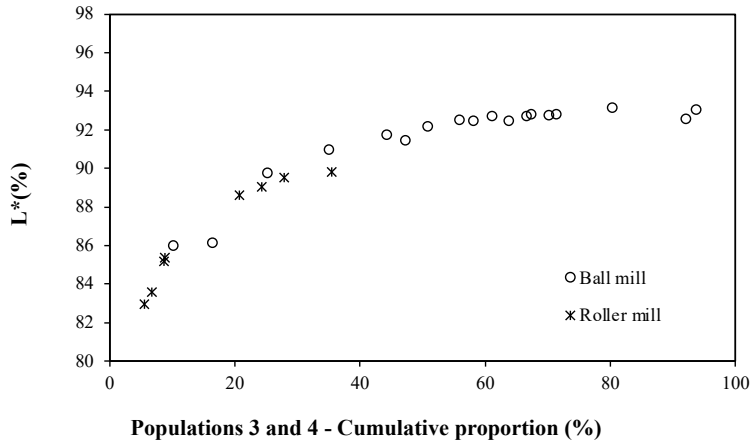

Figure 16. Effect of the cumulative particle proportion of populations 3 and 4 on the lightness of pea powders.

4. Conclusions

Multimodal analysis of particle populations allows us to better describe the mechanisms associated with the fragmentation of yellow pea cotyledon matrices during grinding. These mechanisms evolve differently depending on the grinding conditions. They can be

monitored by analyzing the particle size distribution curves through the proportion and intensity of different peaks. The characterization of isolated populations and their impact on the properties of the whole powder would allow us to study the process–structure–function relationship of powders. The aim is to pilot the generation of functional powders using a reverse engineering approach. Prospective studies will seek to consolidate the proposed hypotheses on mechanisms through a more detailed analysis of the state of the constituents and the quality of the powders generated as a function of the grinding conditions.

Author Contributions: L.K. (conceptualization, methodology, investigation, data curation, writing, original draft preparation, writing review and editing, and supervision); R.B., A.R. and B.C. (conceptualization, methodology, investigation, writing, writing review, and supervision). All authors have read and agreed to the published version of the manuscript.

Funding: This research is funded by a ministerial grant from the University of Montpellier.

Institutional Review Board Statement: Not applicable.

Informed Consent Statement: Not applicable.

Data Availability Statement: The data presented in this study are available on request from the corresponding author.

Acknowledgments: The authors wish to thank Cécile Sotto for her precious help with the BET measurements. The authors thank the PLANET facility (https://doi.org/10.15454/1.5572338990609338E12) run by the IATE joint research unit for providing process experiment support.

Conflicts of Interest: The authors declare no conflicts of interest.

References

1. Siddiq, M.; Uebersax, M.A. Dry beans and pulses production and consumption—An overview. In *Dry Beans Pulses Production, Processing and Nutrition*, 1st ed.; Siddiq, M., Uebbersax, M.A., Eds.; John Wiley Son Inc.: Oxford, UK, 2013; pp. 1–22. [CrossRef]
2. Thakur, S.; Scanlon, M.G.; Tyler, R.T.; Milani, A.; Paliwal, J. Pulse flour characteristics from a wheat flour miller's perspective: A comprehensive review. *Compr. Rev. Food Sci. Food Saf.* **2019**, *18*, 775–797. [CrossRef] [PubMed]
3. Scanlon, M.; Thakur, S.; Tyler, R.; Milani, A.; Der, T.; Paliwal, J. The critical role of milling in pulse ingredient functionality. *Cereal Foods World* **2018**, *63*, 201–205.
4. Bourré, L.; Frohlich, P.; Young, G.; Borsuk, Y.; Sopiwnyk, E.; Sarkar, A.; Malcolmson, L. Influence of particle size on flour and baking properties of yellow pea, navy bean, and red lentil flours. *Cereal Chem.* **2019**, *96*, 655–667. [CrossRef]
5. Price, C.; Kiszonas, A.M.; Smith, B.; Morris, C.F. Roller milling performance of dry yellow split peas: Mill stream composition and functional characteristics. *Cereal Chem.* **2021**, *98*, 462–473. [CrossRef]
6. Sridharan, S.; Meinders, M.B.; Bitter, J.H.; Nikiforidis, C.V. Pea flour as stabilizer of oil-in-water emulsions: Protein purification unnecessary. *Food Hydrocoll.* **2020**, *101*, 105533. [CrossRef]
7. Monnet, A.F.; Jeuffroy, M.H.; Villemejane, C.; Michon, C. Effect of the order of incorporation of cake ingredients on the formation of batter and the final properties: Contribution of the addition of pea flour. *J. Food Sci. Technol.* **2021**, *58*, 4252–4262. [CrossRef] [PubMed]
8. Maskus, H.; Bourre, L.; Fraser, S.; Ashok, S.; Malcolmson, L. Effects of grinding method on the compositional, physical, and functional properties of whole and split yellow pea flours. *Cereal Foods World* **2016**, *61*, 59–64. [CrossRef]
9. Pelgrom, P.J.; Vissers, A.M.; Boom, R.M.; Schutyser, M.A. Dry fractionation for production of functional pea protein concentrates. *Food Res. Int.* **2013**, *53*, 232–239. [CrossRef]
10. Du, S.K.; Jiang, H.; Yu, X.; Jane, J.L. Physicochemical and functional properties of whole legume flour. *LWT-Food Sci. Technol.* **2014**, *55*, 308–313. [CrossRef]
11. Vitelli, M.; Rajabzadeh, A.R.; Tabtabaei, S.; Assatory, A.; Shahnama, E.; Legge, R.L. Effect of hammer and pin milling on triboelectrostatic separation of legume flour. *Powder Technol.* **2020**, *372*, 317–324. [CrossRef]
12. Gu, Z.; Jiang, H.; Zha, F.; Manthey, F.; Rao, J.; Chen, B. Toward a comprehensive understanding of ultracentrifugal milling on the physicochemical properties and aromatic profile of yellow pea flour. *Food Chem.* **2021**, *345*, 128760. [CrossRef]
13. Sivakumar, C.; Chaudhry, M.M.A.; Nadimi, M.; Paliwal, J.; Courcelles, J. Characterization of roller and Ferkar-milled pulse flours using laser diffraction and scanning electron microscopy. *Powder Technol.* **2022**, *409*, 117803. [CrossRef]
14. Cheng, F.; Ding, K.; Yin, H.; Tulbek, M.; Chigwedere, C.M.; Ai, Y. Milling and differential sieving to diversify flour functionality: A comparison between pulses and cereals. *Food Res. Int.* **2023**, *163*, 112223. [CrossRef] [PubMed]
15. Thomas, J.; Gargari, S.G.; Tabtabaei, S. Tribo-electrostatic separation of yellow pea and its optimization based on milling types and screen sizes. *Powder Technol.* **2023**, *415*, 118169. [CrossRef]

16. Motte, J.C.; Tyler, R.; Milani, A.; Courcelles, J.; Der, T. Pea and lentil flour quality as affected by roller milling configuration. *Legume Sci.* **2021**, *3*, e97. [CrossRef]
17. Pelgrom, P.J.; Boom, R.M.; Schutyser, M.A. Functional analysis of mildly refined fractions from yellow pea. *Food Hydrocoll.* **2015**, *44*, 12–22. [CrossRef]
18. AACC Methods. *26-32.01-Experimental Milling—Batch Method for Soft Wheat*, 11th ed.; Approved Methods of Analysis; Cereals & Grains Association: St. Paul, MN, USA, 2009.
19. Pujol, R.; Létang, C.; Lempereur, I.; Chaurand, M.; Mabille, F.; Abecassis, J. Description of a micromill with instrumentation for measuring grinding characteristics of wheat grain. *Cereal Chem.* **2000**, *77*, 421–427. [CrossRef]
20. Hausner, H.H. *Friction Conditions in a Mass of Metal Powder*; Polytechnic Inst. of Brooklyn, Univ. of California: Los Angeles, CA, USA, 1967.
21. Bordeaux, D.; Bénézet, J.C.; Benhassaine, A. Les mécanismes de la rupture au cours du broyage de grains de blé dur. 2007. Available online: https://hal.science/hal-00311859 (accessed on 2 April 2024).
22. Kornet, C.; Venema, P.; Nijsse, J.; van der Linden, E.; van der Goot, A.J.; Meinders, M. Yellow pea aqueous fractionation increases the specific volume fraction and viscosity of its dispersions. *Food Hydrocoll.* **2020**, *99*, 105332. [CrossRef]
23. Möller, A.C.; van der Padt, A.; van der Goot, A.J. From raw material to mildly refined ingredient–Linking structure to composition to understand fractionation processes. *J. Food Eng.* **2021**, *291*, 110321. [CrossRef]
24. Ajala, A.; Kaur, L.; Lee, S.J.; Singh, J. Influence of seed microstructure on the hydration kinetics and oral-gastro-small intestinal starch digestion in vitro of New Zealand pea varieties. *Food Hydrocoll.* **2022**, *129*, 107631. [CrossRef]
25. Setia, R.; Dai, Z.; Nickerson, M.T.; Sopiwnyk, E.; Malcolmson, L.; Ai, Y. Impacts of short-term germination on the chemical compositions, technological characteristics and nutritional quality of yellow pea and faba bean flours. *Food Res. Int.* **2019**, *122*, 263–272. [CrossRef] [PubMed]
26. Pernollet, J.C. Protein bodies of seeds: Ultrastructure, biochemistry, biosynthesis and degradation. *Phytochemistry* **1978**, *17*, 1473–1480. [CrossRef]
27. Tyler, R.T. Impact milling quality of grain legumes. *J. Food Sci.* **1984**, *49*, 925–930. [CrossRef]
28. Maaroufi, C.; Melcion, J.P.; De Monredon, F.; Giboulot, B.; Guibert, D.; Le Guen, M.P. Fractionation of pea flour with pilot scale sieving. I. Physical and chemical characteristics of pea seed fractions. *Anim. Feed Sci. Technol.* **2000**, *85*, 61–78. [CrossRef]
29. Monnet, A.F.; Laleg, K.; Michon, C.; Micard, V. Legume enriched cereal products: A generic approach derived from material science to predict their structuring by the process and their final properties. *Trends Food Sci. Technol.* **2019**, *86*, 131–143. [CrossRef]
30. Bordeaux, D.; Bénézet, J.C.; Benhassaine, A. Étude systémique du broyage du blé dur par un broyeur à boulets. *Ind. Des Céréales* **2006**, *149*, 5–10.
31. Davydova, N.I.; Leont'Ev, S.P.; Genin, Y.V.; Sasov, A.Y.; Bogracheva, T.Y. Some physico-chemical properties of smooth pea starches. *Carbohydr. Polym.* **1995**, *27*, 109–115. [CrossRef]
32. Assatory, A.; Vitelli, M.; Rajabzadeh, A.R.; Legge, R.L. Dry fractionation methods for plant protein, starch and fiber enrichment: A review. *Trends Food Sci. Technol.* **2019**, *86*, 340–351. [CrossRef]
33. Kim, J.M.; Shin, M. Effects of particle size distributions of rice flour on the quality of gluten-free rice cupcakes. *LWT-Food Sci. Technol.* **2014**, *59*, 526–532. [CrossRef]
34. Ahmed, J.; Taher, A.; Mulla, M.Z.; Al-Hazza, A.; Luciano, G. Effect of sieve particle size on functional, thermal, rheological and pasting properties of Indian and Turkish lentil flour. *J. Food Eng.* **2016**, *186*, 34–41. [CrossRef]
35. Bala, M.; Handa, S.; Mridula, D.; Singh, R.K. Physicochemical, functional and rheological properties of grass pea (*Lathyrus sativus* L.) flour as influenced by particle size. *Heliyon* **2020**, *6*, e05471. [CrossRef] [PubMed]